

On the Feasibility of Fingerprinting Collaborative Robot Traffic

Cheng Tang
University of Waterloo
Waterloo, Ontario, Canada
cheng.tang@uwaterloo.ca

Diogo Barradas
University of Waterloo
Waterloo, Ontario, Canada
diogo.barradas@uwaterloo.ca

Urs Hengartner
University of Waterloo
Waterloo, Ontario, Canada
urs.hengartner@uwaterloo.ca

Yue Hu
University of Waterloo
Waterloo, Ontario, Canada
yue.hu@uwaterloo.ca

ABSTRACT

This study examines privacy risks in collaborative robotics, focusing on the potential for traffic analysis in encrypted robot communications. While previous research has explored low-level command recovery, our work investigates high-level motion recovery from command message sequences. We evaluate the efficacy of traditional website fingerprinting techniques (k-FP, KNN, and CUMUL) and their limitations in accurately identifying robotic actions due to their inability to capture detailed temporal relationships. To address this, we introduce a traffic classification approach using signal processing techniques, demonstrating high accuracy in action identification and highlighting the vulnerability of encrypted communications to privacy breaches. Additionally, we explore defenses such as packet padding and timing manipulation, revealing the challenges in balancing traffic analysis resistance with network efficiency. Our findings emphasize the need for continued development of practical defenses in robotic privacy and security.

1 INTRODUCTION

In recent years, robotics has rapidly evolved to become an integral part of many industries and domains, including manufacturing, healthcare, transportation, and even personal use, in a fully autonomous fashion or shared-control fashion such as teleoperation [25]. Among the recent trends in robotic applications, the healthcare and service sectors have seen increased options, thanks to the advent of collaborative robots that can be used in close contact with humans. Examples of robotic applications such as surgical assistants [16] and patient care [35] have advantages such as increased dexterity and precision [17], and applications in home assistance [52] can guarantee independent living and healthy aging.

However, the integration of robotics in direct interaction with humans also introduces significant privacy concerns [44]. The continuous communication between robotic systems and control interfaces, often encrypted yet susceptible to traffic analysis (i.e., the examination of communication metadata like the volume of communication or the frequency of packet exchanges), can enable malicious actors to infer critical information about the end users (e.g. a patient’s health status, specific medical procedures being performed, or even daily routines in care settings). Such breaches not only pose risks to individual privacy but can also compromise trust in adopting robotic systems. The privacy threat is not just a matter of unauthorized data access; it extends to the potential misuse of

sensitive information, which can have far-reaching implications for end-users and service providers [11].

Previous work [44] has begun exploring the potential leakage of robotic operations through the analysis of encrypted traffic, focusing on the recovery of low-level commands sent to a robot. This research primarily concentrated on reconstructing high-level motion from low-level movements by analyzing features such as packet lengths and inter-arrival times. While prior research is tailored specifically to teleoperated robots and relies on deep learning to classify low-level motions within certain setups, we employ signal processing to extract command messages. This approach is applicable to any robot providing an API, as long as the traffic pattern is known and can be utilized to identify similar pattern. By classifying actions based on extracted temporal dependencies through classical machine learning, our model requires few data samples and could potentially be extended across various robotic systems, given the inherent nature of the tasks they perform.

We study potential threats arising from traffic analysis in robotic operations, focusing our analysis on the traffic generated by collaborative robots. We start by leveraging established traffic analysis techniques used in the related domain of website fingerprinting, such as k-FP [22], KNN [51], and CUMUL [36], to extract features from our network traces and classify robot actions. However, we find that these methods are unable to account for detailed temporal relationships between sequences of command messages, critical for identifying robotic actions (Section 5).

To address these shortcomings, we introduce a novel traffic classification approach based on signal processing techniques (Section 6). Our core insight is that distinct robot operation commands generate specific traffic sub-patterns which can be accurately identified through the application of signal correlation and convolution techniques, offering a closer understanding of robotic actions’ traffic. Further, we develop and evaluate custom traffic analysis defenses tailored to robot operation environments. Drawing inspiration from existing traffic analysis defenses, we implement two metadata obfuscation mechanisms based on padding and on the manipulating packet timings. We quantify the performance overhead introduced by various defense configurations while assessing their effectiveness in reducing the success of traffic analysis techniques.

In our evaluation, we conduct experiments over a network traffic dataset comprising four robotic actions that were manually generated. The results of our experiments show that our signal processing-based classification technique is able to identify these actions with an accuracy of 97%, thus revealing that adversaries

might be able to infer sensitive robotic actions from encrypted network traffic alone. In turn, our experiments with traffic analysis defenses suggest that balancing traffic analysis resistance with network efficiency is challenging in practical settings, casting the need for additional work towards the development of practical defenses that can be widely applied to the robot operation scenario.

2 BACKGROUND

2.1 Control Interfaces in Robotics

In the realm of robotics, the control interfaces primarily fall into two categories: *script-based control* and *teleoperation*. These interfaces are distinguished by their approaches to robot control, the unique traffic patterns they generate, and the potential privacy risks they pose, especially in encrypted communication settings. Our focus in this study is on script-based robot control, which we find particularly pertinent to the context of collaborative robotics.

Script-based control. In this model, the robot operates based on a set of predefined rules and commands, which are typically programmed into scripts. The robot autonomously executes these commands, requiring minimal to no human intervention once the script starts running. This approach is akin to a user computer communicating with the robot’s controller, where the controller’s role is to send command messages for the robot to interpret and act upon. For example, in a domestic collaborative robot setting, script-based control could involve a robot arm programmed to perform routine household tasks like opening curtains at a specific time or sorting recyclables from trash. The control system ensures that the robot consistently performs these tasks as programmed.

Setup. In script-based control, developers write detailed scripts using programming languages or proprietary software. While these scripts used to contain simple logic that could generate repetitive and predictable sequences, recent advances in robot control, perception, probabilistic approaches, decision-making, and machine learning have led to increasingly complex logic that results in elaborated robot actions that depend on the dynamic environment and interactions with other parties (robot, humans). In script-based control, scripts are typically run on the robot’s controller, with commands sent to the robot’s onboard computer for execution. The network serves as the communication channel for command transmission and feedback. For example, in a pick-and-place operation, feedback might include vision, location, and object type, all crucial for the robot’s task execution. This feedback is generated by the onboard computer, communicated back to the controller, and affects the subsequent commands.

Teleoperation. Teleoperation enables operators to remotely control robotic systems in distinct ways. One is the primary-secondary model, where the robot (secondary) mimics the actions performed by the human operator (primary). The other approach involves the operator sending high-level commands to the robot, which are then executed autonomously without direct mimicry.

Setup. In teleoperation, commands are transmitted from a human-operated control device to the robot. The setup often involves sophisticated interfaces, including joysticks, gloves, or even virtual reality gear, which translate human movements into robot actions. Feedback mechanisms, such as sensory data or video streams, are

common to provide the operator with situational awareness. The major difference between this control modality and the script-based one consists of the human-in-the-loop control and the feedback being processed by the human operator rather than by the control program itself, meaning that the sensory data returned may not be directly used by the program of the robot.

Privacy implications. In both control modalities, network traffic manifests as sequences of command messages (albeit different types due to the difference in interfaces), which can be structured and exhibit recognizable patterns. An adversary conducting traffic analysis could potentially identify specific tasks or routines by observing and identifying patterns that emerge from communication metadata like the timing, frequency, and lengths of network packets. In the case of script-based control, the adversary may be able to identify routine procedures by inferring robot actions derived from high-level programming logic, while in the case of teleoperation, they may infer the remote operator’s intents and actions. For instance, in the sensitive context of healthcare and caregiving, a repetitive sequence may indicate a routine medical procedure, and certain sequences of specific types of messages may indicate sensory information (e.g. heart rate, blood pressure) needed to evaluate the health status of a patient, inadvertently revealing patient information or healthcare practices.

2.2 The Kinova Robotic Arm & APIs

The Kinova robotic arm, particularly its Gen3 model, represents a significant advancement in collaborative robotics, healthcare, and research [10, 18, 37]. The Gen3 model is a commercially available robotic arm, accessible not only to industries and research institutions but also to individual consumers. This wide availability would also enable adversaries to potentially have access to these robots and study their APIs.

The Gen3 arm provides a rich API, offering developers a comprehensive toolkit of protocols, functions, and libraries for both high-level command dispatch and low-level control of individual components. In line with cybersecurity best practices, communication with the Kinova robotic arm is secured using encrypted channels, such as TLS, to protect the integrity and confidentiality of transmitted data. Script-based control of the arm can use either the high-level or low-level APIs, catering to a wide range of tasks.

In our study, we primarily focus on the high-level controls provided by the Kinova API, enabling the analysis of command sequences typically used for more abstract and complex tasks.

High-level API controls. The Kinova robotic arm’s API facilitates an abstraction layer through its high-level controls, allowing developers to command complex movements and sequences with relative ease. As an example, for a “pick and place” task, the robot’s controller (an external computer), might receive a sequence of Cartesian movement command messages (movements of the robot end-of-tool in the 3D space) messages to navigate to the target object, followed by a gripper movement command message to grasp the object. The controller then receives another set of command messages to move to the new location and release the object with a final gripper command. These high-level command messages translate into a standardized set of instructions sent from the controller to the robotic arm. Given the abstract nature of these commands,

they typically result in a uniform and consistent network traffic pattern (see Section 4) since each high-level command corresponds to a specific sequence of movements, which in turn generates a predictable series of data packets over the network.

Low-level API controls. On the other end of the spectrum, the API’s low-level controls offer a more granular interaction with the robotic arm. Developers have the ability to manipulate individual joints, receive sensor feedback in real-time, and implement custom control algorithms. For instance, in a task such as picking and placing, the low-level controls enable fine adjustment of the robot’s wrist and fingers to accurately handle and reposition the target object. This level of control introduces a larger variability in the network traffic, as the data packets are now closely tied to the multiple adjustments and feedback loops necessary for precise movements. Each adjustment, sensor reading, and feedback response contributes to a complex and nuanced network traffic pattern. Note that there is a one-to-one mapping between API invocations and commands sent to the robotic arm. Each API call directly translates into a specific command or set of commands, which are then communicated to the arm. This direct relationship ensures that each action initiated via the API results in a corresponding response from the robot, creating a traceable link between the software interactions and the physical movements of the robotic arm.

Privacy implications. The interaction between the controller and the Kinova robotic arm generates network traffic patterns that are dictated by the architecture and operation of the API. Unfortunately, these patterns can inadvertently expose sensitive information about the environment in which the robotic arm is operating or even enable an adversary to deduce the specific tasks it is performing. The information extracted from the high-level API controls is broadly equivalent to the information that could be derived from script-based control methods (see Section 2.1). This similarity arises because both high-level API controls and script-based control typically involve predefined sets of commands or rules that defines commands. In both cases, the resulting network traffic patterns are influenced by the sequence and nature of these predefined commands. Therefore, while high-level API controls offer more abstracted interactions with the robot, the privacy implications and potential for traffic analysis remain similar to those encountered with script-based robotic control methods.

2.3 Encrypted Traffic Fingerprinting

Encrypted traffic fingerprinting is a general term for describing a traffic analysis technique based on the examination of the metadata of encrypted traffic [2, 15]. More concretely, by inspecting traffic characteristics like overall communication volume, packet sizes, or packet timing intervals, an eavesdropper can build a profile of the network behavior of some Internet-based application under a specific workload (i.e., a traffic fingerprint), and then re-identify the occurrence of the same workload by matching its fingerprint.

As seen in the above sections, fingerprinting techniques (and defenses against them) are also expected to become particularly relevant in the context of robot operation traffic.

Reconstruction of robot operations from encrypted traffic. Shah et al. [44] discuss reconstructing robot high-level movements from lower-level movements in teleoperation scenarios, where an

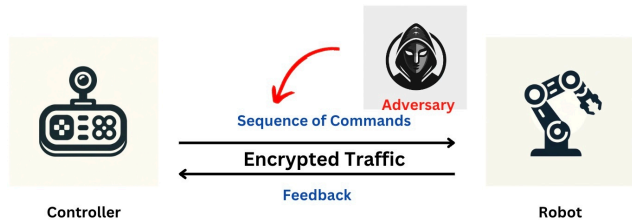


Figure 1: Depiction of our threat model.

operator directly controls the robot using a movement controller. This approach contrasts with our focus, which lies on script-based applications and reconstructing traffic patterns by analyzing sequences of command messages. Shah et al.’s methodology, which employs a simple neural network with a single hidden layer to analyze encrypted traffic data for identifying robot movements and reconstructing workflows, is tailored to teleoperated systems with a dynamic operator control. This differs from our context of scripted robotic actions, making their approach not directly applicable to our experiments due to these distinct setups involved.

We will discuss other traffic analysis scenarios and methods in Section 9, offering a broader perspective on the diverse approaches within the domain of traffic fingerprinting.

3 METHODOLOGY

This section describes our evaluation methodology. First, we describe our threat model and our experimental testbed. Then, we detail the metrics used to evaluate the success of attacks and defenses applied to robot control traffic.

3.1 Threat Model

An overview of our threat model is depicted in Figure 1, where we assume the existence of an adversary who is able to passively listen to the communication between a robot and its controller. We assume the controller and the robot to be located in different network locations. As an example, considering a healthcare scenario, the robot could be located in a user’s home while being remotely controlled by an operator within a hospital facility.

The adversary’s goal is identifying the actions performed by the robot through the analysis of the traffic patterns generated by the robot control operation, which includes the exchange of controller commands and robot feedback. We assume that the adversary may also be interested in recognizing more fine-grained information about the robot actions, such as identifying the exact commands sent to the robot that enable it to perform a given action. This level of insight could enable the adversary to predict the robot’s activities in near real-time, which could cause a significant breach of operational security. As in our running example considering sensitive healthcare contexts, this could potentially lead to the unintended exposure of patient-specific information through the analysis of repeated command patterns corresponding to specific medical procedures. For instance, a sequence of commands unique to a particular type of therapy could inadvertently reveal the treatment regimen of a patient, or regular checks at certain times may disclose the schedule of medication administration, underlining the criticality of thwarting such adversarial efforts.

We assume that the adversary has the following main capabilities: First, the adversary has their own robot and controller, whose model/version is identical to the one used by the target user. This allows the adversary to use its own robot (and unrestricted API access) to study traffic patterns. This level of access provides them with a comprehensive understanding of potential traffic patterns, thus offering them a strategic advantage in predicting and interpreting traffic flows. Second, the adversary is able to leverage multiple techniques to analyse traffic flows towards generating features that can help characterize traffic traces (e.g., deriving summary statistics, or deriving information about well-defined patterns through signal processing operations). Finally, the adversary can make use of machine learning techniques, which can help it interpret the command sequences issued to the robot and ultimately identify actions issued via the controller.

We also assume that the adversary is limited in its operation. Specifically, the adversary is unable to break the cryptographic primitives used for securing the control channel, and the adversary has no control over the endpoints engaged in communication. Thus, we assume that both the controller and the robotic arm are trusted and remain free from adversarial compromises (e.g., via malware) that could help the adversary in collecting additional information about the commands executed by the robot.

3.2 Experimental Setup

Our experimental testbed emulates a real-world robot operation scenario. Below, we elaborate on the specific details of our setup and evaluation settings:

Hardware and software configuration. Our experiments leverage a Kinova Robotic Arm Gen3 [26] (depicted in Appendix A – Figure 14), which remotely receives commands and returns feedback to a workstation acting as a controller. The workstation acting as a controller runs Ubuntu 20.04 LTS and is configured with a 2.40 GHz Intel Core i7-8700T CPU and 32GB RAM. The workstation and the robotic arm are interconnected using Ethernet cabling to ensure a reliable communication. We use the Kinova API v2.3.0 for controlling the robotic arm and generating command patterns, configuring it to enable TLS-based encrypted communication between the robot and the controller. To capture the network traffic for our analysis, we use `tcpdump` on the controller workstation to record the encrypted data exchanges between the robot and the controller.

Robot actions dataset. For conducting our study, we gather a set of network traces generated when operating the robot to perform four different kinds of actions, including: a) picking up and placing an object, b) pouring water, c) turning on a switch, and d) pressing a key. We provide a depiction of the robotic arm while performing each of these actions in Figure 2. The actions share a certain degree of similarity; for instance, both pouring water and turning on a switch involve fluid motions and subtle changes in the robot’s articulation, which could be reflected in the traffic patterns as similar command message sequences, making it challenging to distinguish between them accurately. The duration of each trace also varies significantly across actions to capture cases where users might take different times to complete the same action. However, all our samples are bounded to a minimum and maximum completion time of 5 and 30 seconds, respectively.

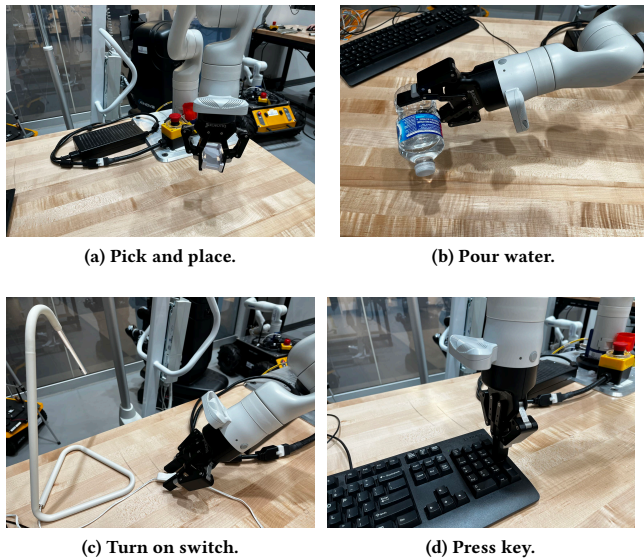


Figure 2: The Kinova robotic arm executing four actions.

We obtain our dataset by manually instructing the robot to execute the four above actions, and collecting the network traffic exchanged between the robot and the controller. We collect 50 samples for each action, for a total of 200 samples. The robot executes actions according to a set of predefined rules that an operator writes in scripts, towards completing certain tasks. We note, however, that the collection of this data is still bound to the physical operation of the robot, which we cannot easily parallelize (apart from using additional robots, but which were unavailable to us).

The catalog of commands we execute includes different combinations of Cartesian motions, the opening/closing of a gripper claw, and adjustments of the gripper’s speed. This flexibility captures a multitude of real-world scenarios where different operators may script the completion of an identical task with a different number of high-level commands or change their order. We leave the exploration of other approaches to generate command traffic sequences automatically (including generative adversarial networks [55] or stable diffusion models [24]) to future work.

Considered traffic analysis attacks. For showcasing the potential threats of traffic analysis attacks on robot control traffic, we leverage the open-source implementations [19] of attacks used in the context of website fingerprinting, including k-FP [22], kNN [51], and CUMUL [36]. These attacks rely on manually-engineered traffic features, which make heavy use of summary statistics and have low data collection requirements, making them suitable to our setting.

ML models’ evaluation. The machine learning models employed in our study are trained and tested using stratified 10-fold cross-validation to mitigate the impacts of bias in the dataset. We refrain from using an additional validation set since we use all machine learning models with their default hyperparameter configurations.

3.3 Metrics

We employ the following metrics when evaluating our traffic analysis attacks and defenses on robot control traffic:

Attack evaluation metrics. We leverage accuracy as our main metric to assess attack performance. Accuracy is defined as the ratio of the number of correctly classified observations to the total number of observations. We also make use of confusion matrices to visualize attack performance across the multiple action classes by inspecting the distribution of correct and incorrect predictions.

Defense evaluation metrics. When evaluating the defense mechanisms implemented to protect against traffic analysis, we primarily focus on two aspects: the reduction of an attack’s *accuracy* (effectiveness), and the impact of the defense on the robot’s performance (efficiency). We measure the efficiency of the defense through the *bandwidth utilization* and *latency increase* experienced by the robot’s activities. To compute bandwidth utilization overheads, we compare the amount of additional data exchanged due to the defense. To compute latency impacts, we compute the delays introduced in the communication between the robot and the controller, and assess the potential impacts of such delays on the correct operation of the robot and its ability to complete a designated task.

4 CHARACTERIZATION OF ROBOT ACTIONS

In this section, we characterize the different actions composing our dataset, showcasing both the inter-class and intra-class variability of the generated traffic traces.

Individual commands have stable traffic signatures. Each row of Figure 3 shows two different network traces for a Cartesian command and a gripper movement command, respectively. We can see that different executions of the same command result in similar traffic patterns, but that these patterns also differ amongst each different kind of command. In more detail, Cartesian commands involve moving the robot arm in three-dimensional space and typically span a shorter period of time compared to gripper position commands. These Cartesian movements usually elicit a longer feedback packet from the robot arm, indicative of the arm’s positional adjustments in a 3D space. In contrast, gripper position command messages control the opening and closing of the robot’s gripper, and consist of packets just over 100 bytes in either direction. Each of these packets corresponds to an adjustment in the gripper’s position. Appendix B presents details on additional commands, including angular motion commands and gripper speed commands, which follow a similar trend to the above examples.

Different actions result in different traffic patterns. Figure 4 shows example traffic patterns for the four classes of actions included in our dataset, showcasing both incoming and outgoing traffic from the point of view of the controller workstation. At a high level, we can see that each different action generates a disparate traffic pattern. For instance, the pick and place action generally involves at least two distinct gripper command messages, before and after the act of picking and placing an object. This is reflected in the traffic (Figure 2a) as two dense clusters of gripper position or speed command messages, indicating the gripper’s motion to open and close. Despite two actions being markedly dissimilar, the traces generated by the pour water action (Figure 2b) exhibit some similarities tied to specific commands that instruct the closing of the gripper to grab the bottle and opening it after pouring.

In turn, actions such as turning on a switch (Figure 2c) or pressing a key (Figure 2d) typically involve a tapping motion, which

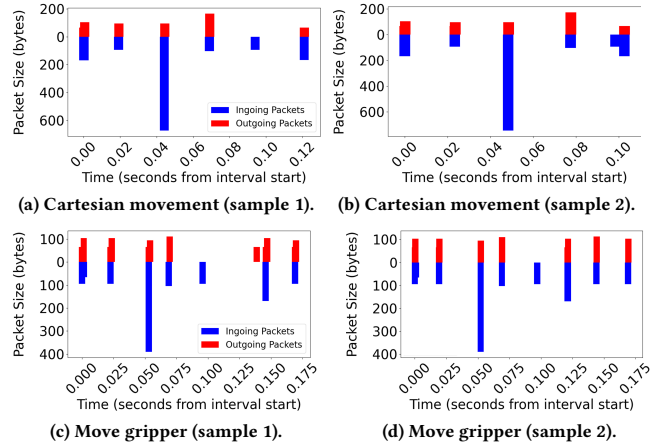


Figure 3: Network traces for two kinds of commands. Note that the x-axes use different scales.

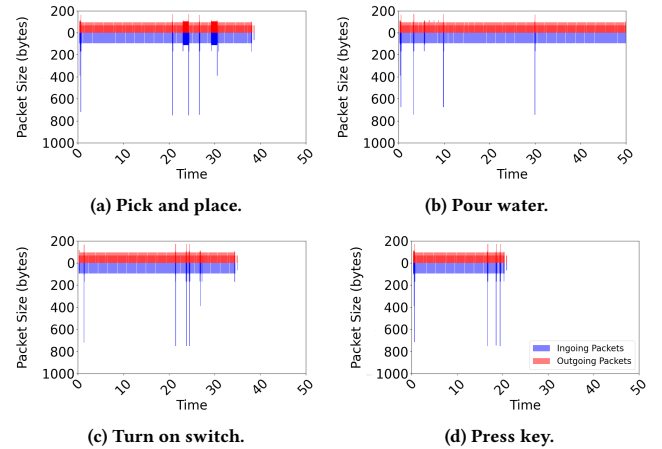
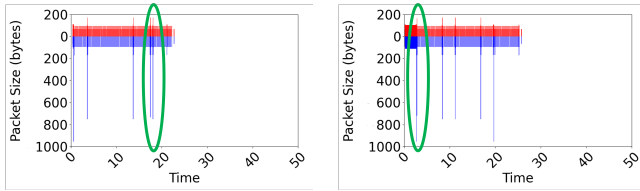


Figure 4: Examples of actions’ packet lengths over time.

requires the robot to close the gripper beforehand. These actions do not necessitate additional gripper motions afterwards, although the gripper may open if required by subsequent tasks. The timing between Cartesian command messages also offers intricate details; tapping motions are usually swift, leading to shorter intervals between command messages. Other noteworthy detail includes the observation of interleaved occurrence of different commands. For instance, in the pick and place action, we can observe the presence of Cartesian command message between two gripper command messages, as seen in Figure 4c, around the 25 second mark. These temporal dependencies that are characteristic to each action may provide actionable information for building an effective classifier.

Traffic patterns for a given action are highly variable. Figure 5 presents two variations of the turn on switch action, showcasing that the traffic patterns for a given action can also be distinct and challenging to recognize by simple observation. However, upon closer inspection, the composition of individual commands sent to the robot can help us identify an action, such as the short period of time between two Cartesian command messages, as circled in green in Figure 5a, and a gripper command (closing the gripper)



(a) Turn on switch (sample 1).

(b) Turn on switch (sample 2).

Figure 5: Examples of “turn on switch” network traffic traces.

at the beginning of the action to prepare for the tapping motion, immediately followed by a Cartesian command message, as circled in green in Figure 5b.

The results of our characterization suggest that there are multiple sources of information in robot traces that may be leveraged for enabling their accurate classification. In the next sections, we experiment with different traffic classification approaches and assess whether these enable the successful identification of robot actions.

5 EXPLOITING KNOWN ATTACKS FOR ROBOT ACTION IDENTIFICATION

Multiple classifiers have been proposed to assess the feasibility of performing traffic fingerprinting. Perhaps the most well-studied context is website fingerprinting, where researchers have proposed multiple ways to extract features that can be used to feed machine learning classifiers aimed at identifying visited webpages.

In this section, we explain how popular classifiers operate and detail the rationale behind each of their feature sets. Then, we conduct a comparative analysis of the success of each of these classifiers in the robot operation traffic fingerprinting scenario.

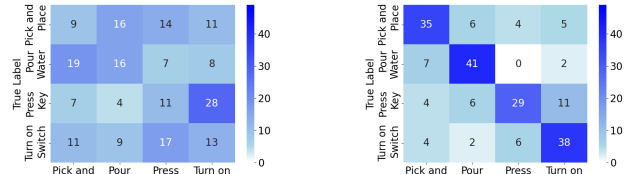
5.1 ML-based Website Fingerprinting Attacks

We describe three prominent classifiers that have been used for successful traffic analysis attacks in the context of website fingerprinting. We also provide an overview of the used feature sets.

k-NN [51]. The feature set for this attack comprises the total transmission bandwidth and elapsed time, the total number of incoming and outgoing packets, unique packet lengths, packet ordering and bursts, and the lengths of the first 20 packets in each direction. The attack leverages the k-Nearest Neighbors classifier, where different features are attributed disparate weights.

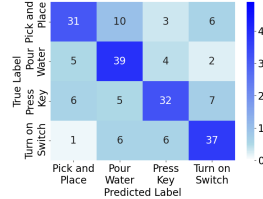
CUMUL [36]. The feature set used in this attack includes the total number of incoming and outgoing packets, total bandwidth used in each direction. Additionally, 100 features are generated from the cumulative sum of packets’ sizes of the connection at different points in a network trace. The attack leverages a Support Vector Machine with an RBF kernel.

k-FP [22]. This attack introduces a combination of features used in previous attacks with novel traffic characteristics, leading to a systematic analysis of 150 traffic features. The classifier works by building a fingerprint for each web page using a modification of the Random Forest algorithm. Then, the attack employs the k-Nearest Neighbors classifier to predict web page accesses.



(a) K-NN.

(b) CUMUL.



(c) K-FP.

Figure 6: Confusion matrices for existing attacks.

5.2 Attacking Robot Operation Traffic

We now present our main findings after applying the classifiers introduced above for attempting the identification of robot actions issued via the controller.

ML-based website fingerprinting attacks fail to correctly identify robot actions. Our experiments reveal that the attacks introduced in the previous section obtain a poor accuracy in correctly identifying the robot’s actions in the dataset. Specifically, k-FP and CUMUL achieve an accuracy close of 69.5% and 71.5%, respectively, while the k-NN attack achieves an accuracy of only 29.5%. Figures 6a–6c depict the confusion matrices for each of the classifiers. We can see that these matrices show a noticeable pattern where the “pick and place” and “pour water” actions seem to more heavily contribute to the classifiers’ mispredictions. These actions are generally more complex than “press key” and “turn on switch”, typically involving a larger number and variety of robotic movements. This complexity often results from the fact that the former actions frequently involve more intricate gripper movements that use gripper speed commands with shorter inter-packet timings.

Why do these attacks fail? The relatively low performance of these attacks in identifying robot actions can be attributed to a set of fundamental differences in the nature of robotics traffic compared to web traffic. As we observed in Section 4, the robotic actions considered in our work generate highly variable traffic patterns with intricate temporal dependencies that may not be typically present in web traffic. Among these, we highlight nuanced variations in gripper speed and position commands, as well as specific timing intervals between Cartesian command messages. Our results suggest that these dynamic characteristics are not effectively captured by traditional website fingerprinting classifiers, which rely extensively on features based in summary statistics obtained from the entirety of a trace, such as total transmission volume, the frequency distribution of packet lengths, or coarse-grained statistics about inter-packet timing. Importantly, these techniques fail to capture local information in a trace, e.g., the exact timing at which specific robot operation commands are placed.

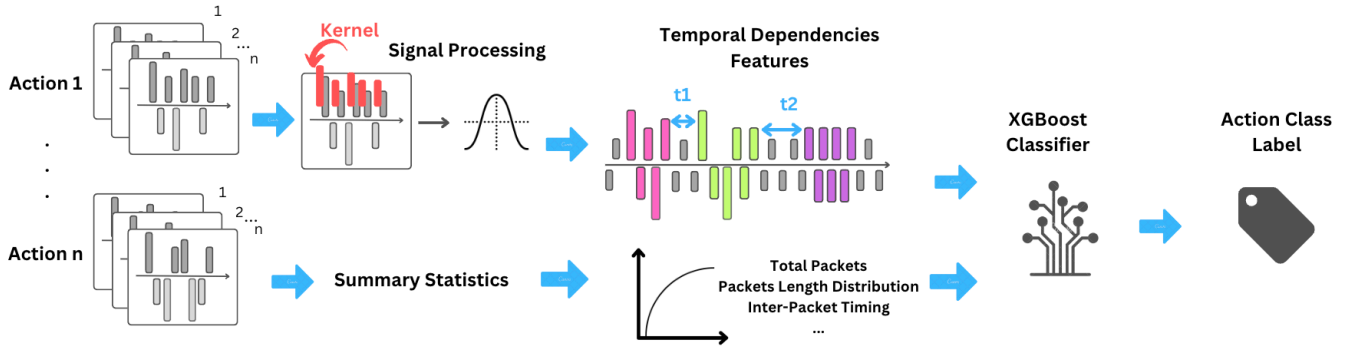


Figure 7: Signal processing-based traffic analysis pipeline for classifying robot actions.

What can we do about it? We argue that the presence of command-specific patterns in robotics traffic, such as visible instances of gripper command messages or distinct intervals between Cartesian commands, demands a more specialized approach for accurate classification. These patterns require a classification approach capable of discerning the temporal dependencies inherent to the different commands composing robotic actions, which seem to be beyond the capabilities of standard classifiers designed for web traffic. In the next section, we depart from the use of well-established classifiers used for fingerprinting network traffic, and introduce a new fingerprinting approach based on signal processing techniques.

6 SIGNAL PROCESSING-BASED ROBOT ACTION IDENTIFICATION

We find that signal processing operations can provide valuable insights when applied to network traffic data, particularly in identifying and characterizing patterns associated with specific commands or actions. At its core, our insight is that each command type defined in the Kinova API (and potentially others, like ROS [38]) results in a distinct traffic pattern when transmitted. This uniqueness arises from various characteristic traits that arise when specific commands are issued, and which manifest themselves in packet sizes, inter-packet intervals, and transmission rates. Consider for instance two distinct Cartesian commands, which instructs the robot to do picking and do pressing, respectively. From Figure 16, which depicts a zoom into the traffic exchanged when these commands are issued, we can see Cartesian commands produce a similar traffic fingerprint despite their different contents.

Given the above, and to understand whether an adversary could enhance its action identification capabilities, we focus on detecting specific events within the network traffic that are directly tied to particular commands executed by the robot. These events serve as building blocks to generate an action’s traffic fingerprint.

Traffic analysis pipeline overview. Figure 7 depicts a bird’s-eye view of our analysis pipeline. Network traces representing different actions start by undergoing a set of signal processing operations (correlation and convolution, c.f. next section) whose results we rely on to build a set of temporal dependency features. These features are then combined with a set of more generic summary statistics obtained from the network traces (inspired in those used by the classifiers analyzed in Section 5). Finally, we use these features

to train (and later test the success of) an XGBoost [7] classifier geared at identifying the actions performed by the robot. We employ XGBoost given that it is known to outperform other classical machine learning models in both computational speed and model performance, and has been successfully used for traffic analysis [4].

Next, we describe our signal processing approach, detail how it is able to better recognize temporal dependencies and statistical features of robot control traffic, and show how our method is able to achieve a high accuracy in the identification of robot actions.

6.1 Pattern Matching Operations

Our traffic analysis methodology places a large emphasis on the recognition of traffic patterns by leveraging two basic mathematical operations: *correlation* and *convolution*. Next, we provide the necessary background on these operations and then address how their results can be composed into a set of temporal dependencies and statistical features that help us build an accurate classifier.

Convolution. Convolution is a mathematical operation that combines two signals to produce a third, which reflects how the shape of a signal is modified by the other. For two discrete signals $x[n]$ and $h[n]$, their convolution is given by:

$$(x * h)[n] = \sum_{m=-\infty}^{\infty} x[m] \cdot h[n - m]$$

Here, $h[n]$ can be thought of as a “kernel” or “filter” that is slid across $x[n]$. In the realm of traffic pattern recognition, if $x[n]$ is the observed traffic and $h[n]$ is a known pattern, then a significant spike in $(x * h)[n]$ at a particular n indicates the presence of the known pattern in the observed traffic at that point.

Correlation coefficient. The correlation coefficient, often denoted r , quantifies the linear relationship between two signals. For two discrete signals $x[n]$ and $y[n]$, their correlation at lag m is:

$$r[m] = \sum_{n=-\infty}^{\infty} x[n] \cdot y[n + m]$$

The value of $r[m]$ peaks when $x[n]$ and $y[n + m]$ align most closely. In the context of traffic analysis, $x[n]$ could be a known command pattern and $y[n]$ the observed traffic pattern. A peak in $r[m]$ indicates the presence of the command pattern within the observed traffic at lag m . In addition to identifying command patterns, correlation coefficients have also been utilized in various traffic analysis

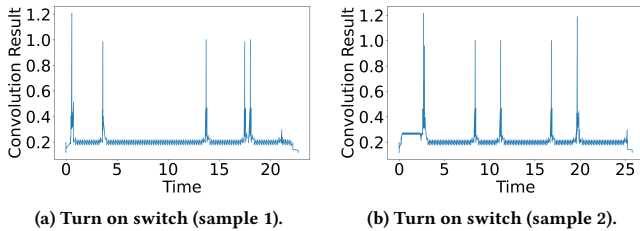


Figure 8: Convolution for two “turn on switch” samples.

tasks, including traffic correlation, to unveil relationships between different sets of network data. Indeed, the approach introduced by Nasr et al. [33] aligns with this idea by analyzing compressed features of network traffic, which could include correlated signal patterns. This method enhances the efficiency of detecting correlations in traffic data, demonstrating its relevance to the correlation coefficient in revealing linear relationships in traffic patterns.

In our experiments, we find that both correlation and convolution play an important role in detecting repetitive patterns within encrypted traffic. While the operations are closely related (they are in fact identical for symmetric $h[n]$), they offer different interpretations and can be used based on the specific requirements of the traffic analysis task at hand.

6.2 Signal Processing-based Traffic Features

In our analysis, we utilize both convolution and correlation-based techniques to extract information on different types of command messages. Some command messages are one-time-only patterns, where convolution is particularly effective. This method allows us to highlight these singular patterns within the broader traffic data. In contrast, other commands are repetitive and may have varying duration; these are better captured using the correlation coefficient to reduce noise and false positives. For instance, we use the correlation coefficient for detecting command messages like gripper speed, where patterns are recurring. Our work primarily focuses on three types of command messages: Cartesian movements, gripper movements, and gripper speed adjustments. Each type presents unique pattern characteristics in network traffic. When introducing a new command message type for detection, we explicitly assess the nature of the command’s traffic pattern. This assessment guides our decision on whether to apply convolution — best for one-time, distinct patterns — or the correlation coefficient, which excels in identifying and analyzing recurring patterns within the traffic data.

Next, we detail two sets of traffic statistics we extract via convolution and correlation-based methods, and then detail how we combine them to produce the final feature set used by our classifier.

Convolution-based statistics. Consider for instance the results of the convolution operation (Figure 8) applied to the two original “turn on switch” action traces depicted in Figure 5. We can see that the convolution result is close to or above 1, meaning that the convolution operation is successfully able to identify significant matches between the observed traffic pattern and the known command pattern. This indicates that the specific features or sequences in the traffic that correspond to the “turn on switch” action are being effectively highlighted by the convolution process.

Metric	Value
Mean Convolution	0.2454
Standard Deviation of Convolution	0.096
Median Convolution	0.2172
25th Percentile of Convolution	0.2163
75th Percentile of Convolution	0.2616
Maximum Convolution	1.2160
Minimum Convolution	0.1181
Skewness of Convolution	6.0470
Kurtosis of Convolution	48.9907
Total Clusters	6
Total Time Span	16.9991
Average Time Gap	3.3998

Table 1: Convolution features (“turn on switch” sample 2).

We note that we used a kernel designed to match the expected traffic pattern generated by the “turn on switch” action. The kernel was crafted based on the characteristic sequence of packet sizes and intervals that we observed in our preliminary analysis for this specific action. Later in Section 6.3, we expand on the implications of selecting an adequate convolution kernel and of finding an adequate threshold for extracting command message information. By convolving this kernel with the observed traffic data, we sought to amplify parts of the signal that match the expected pattern. We determined a threshold to effectively identify instances where the convolution correctly identifies segments in the traffic data that correspond to the “turn on switch” action, based on the predefined kernel. The accurate identification of these segments is instrumental for reconstructing the robot’s actions from the encrypted traffic.

After obtaining the convolution results, we extract a set of statistics from the resulting signal to build a set of convolution-based features. Table 1 presents a summary of the features derived from our analysis. The example in Table 1 shows the features from the second “turn on switch” sample. We observe that there are six Cartesian command messages issued during the sample duration, as reflected in the total of six clusters detected. The table captures and shows the statistics relating to these commands. For example, on average, there is a gap of approximately 4 seconds between each cluster. Additionally, higher-level information such as the total time span and average time gap provides insights into the general dynamics of the action: how frequently the Cartesian command messages are issued and whether they are closely spaced. The maximum convolution value can offer an idea about the number of parameters specified in the Cartesian command message, as this typically results in longer feedback packet sizes.

Correlation-based statistics. Figure 9 depicts the results of the correlation coefficient operation for two original “turn on switch” action traces, previously shown in Figure 5. We can observe a distinct difference in the traffic pattern of the two samples. For instance, the first sample does not exhibit any clusters, suggesting the absence of gripper speed commands, despite a high initial value. Conversely, the second sample displays a prominent cluster at the start, lasting approximately 2 seconds.

To enhance the accuracy of our detection, we establish a criterion where a cluster must consecutively last over 1 second to be considered a positive match. This threshold aligns with the inherent activity of gripper speed commands, which typically persist for a certain duration to maintain a consistent speed or force applied by

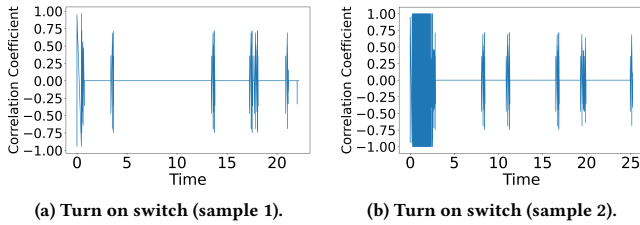


Figure 9: Correlation for two “turn on switch” samples.

the gripper, thereby ensuring that we accurately identify when and for how long these commands are present in the action traffic.

Table 2 provides a summary of the correlation coefficient statistics, offering details similar to those discussed in the convolution analysis. In this context, the cumulative and average lengths of clusters offer additional insights into the duration of commands. We employ the correlation coefficient to identify command messages that exhibit varying recurring patterns (e.g., the gripper speed command) as a means to reduce noise and false positives. By analyzing these statistics, we can ascertain the duration of gripper movements and learn about the extent of ongoing gripper activity.

Our classifier’s feature set. The aforementioned convolution and correlation-based statistics comprise the main fuel for our traffic classifier. Specifically, the detection of each new command message allows us to refine the set of the above statistics with fine-grained information about commands’ temporal dependencies. We obtain features for our model by processing these statistics into a summarized representation of messages’ temporal dependencies.

Concretely, our features include the *average time between clusters*, shedding light on the intervals between command groups; *total number of clusters*, quantifying the diversity of patterns; *total length of all clusters*, giving an aggregate duration of detected patterns; and *average length of clusters*, indicating the typical duration of individual patterns. The *time gaps between consecutive clusters* highlight intervals between patterns, while *skewness and kurtosis* offer insights into their distribution. The *total time span of clusters* provides data about the start of the first to the end of the last cluster, and the *average time gap between clusters* showcases the average intervals between these occurrences. Collectively, these features paint a detailed picture of the robot’s operational patterns, capturing not only the frequency and duration of command messages but also transitions and relationships within them. A complete description of these features can be found in Appendix D – Table 3.

In addition, we also include in our final feature set a collection of common summary statistics extracted from network traffic and that relate to the timing and volume of communication (like the total number of packets exchanged, or average inter-packet timing). We list our full set of features (99 of them) in Appendix E – Listing 1.

6.3 Convolution Parameters

The results of our convolution operation are mostly guided by the choice of two parameters: the convolution kernel, and a threshold for determining the occurrence of a command message. Below, we detail our choice for both parameters.

Convolution kernel. In our experiments, we find that the specific choice of the convolution kernel—a pattern or template used to

Metric	Value
Mean Correlation	-0.0019
Standard Deviation of Correlation	0.5653
Median Correlation	0.0
25th Percentile of Correlation	0.0
75th Percentile of Correlation	5.3926e-17
Maximum Correlation	1
Minimum Correlation	-1
Skewness of Correlation	0.0039
Kurtosis of Correlation	-0.1747
Number of Clusters	1
Total Length of Clusters	2.0910
Average Length of Clusters	2.0910
Total Time Span of Analysis	2.0910
Average Time Gap between Clusters	0

Table 2: Correlation features (“turn on switch” sample 2).

detect similar patterns in the observed data—does not significantly impact the accuracy of the results. Essentially, a kernel represents the overall shape or signature of a particular type of traffic pattern, such as a Cartesian or gripper position command message. For example, a kernel might be derived from a typical pattern of packet sizes and intervals observed for a specific robot command. We test this by using 10 different kernels for each type of command message, each extracted from 10 distinct samples of that command. Despite these variations, the accuracy of our traffic pattern detection remains consistent. This suggests that our method is robust to variations in the kernel, capable of accurately identifying traffic patterns regardless of slight differences in the kernel’s shape.

Convolution threshold. Figure 10a shows the variation in our classifier’s accuracy across different convolution threshold (t) values. The threshold is based on the range of convolution results obtained when the normalized signal is convolved with the normalized kernel, using the normalization factor derived from the kernel itself. A threshold value of 0 means that every positive convolution result, no matter how small, is classified as a Cartesian command message. This can lead to a high rate of false positives, as even minimal similarities between the observed traffic and the kernel are flagged as matches. Conversely, a threshold of 1.3 sets a very high bar for detection, meaning that only very strong matches—those with convolution results exceeding this value—are considered true positives. This strict criterion can increase the likelihood of false negatives, as it may overlook less pronounced but still relevant patterns. In our analysis, we find that a threshold value around 0.9 strikes an optimal balance. This threshold t effectively identifies true Cartesian command messages while minimizing both false positives and false negatives. By setting the threshold at this level, we ensure that only convolution results that are sufficiently high (indicative of a strong match with the kernel pattern) are classified as relevant command messages.

6.4 Evaluation of our Approach

Our traffic analysis pipeline leverages convolution and the correlation coefficient to perform dimensionality reduction, effectively capturing the temporal dependencies in the data, including information about command sequences and their timestamps, which are then explicitly fed into the classifier. According to our experiments, our traffic analysis pipeline achieves an accuracy of 97% for the

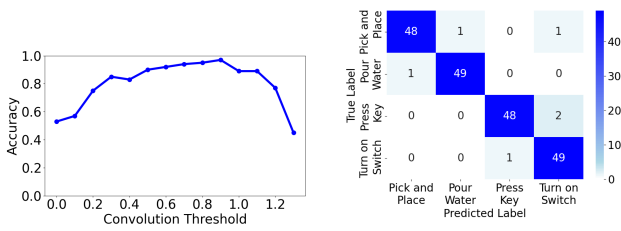


Figure 10: Classification results.

actions dataset. This highlights the potential for network adversaries to compromise the privacy of users through the accurate recognition of robot activities.

Figure 10b depicts the confusion matrix of our classifier on the robot’s actions dataset, allowing for two interesting observations. First, we can see that the classifier occasionally mispredicts the “pick and place” and “pour water” with one another. This misclassification likely stems from the similar sequence of movements shared by these actions, which involve the gripper’s opening and closing motions used for grabbing and placing an object. Second, actions that involve tapping motions, such as pressing a key and toggling a switch, are also occasionally misclassified as each other. Indeed, both classes exhibit quick and sharp motion patterns, which are typical of tapping actions, and thus distinct from the more fluid and prolonged actions of picking, placing, and pouring. Our classifier is able to leverage these unique patterns to more accurately differentiate between these two sets of actions.

Feature importance. We analyzed the contribution of each feature to the classifier’s performance and observed that the top 20 most important features comprise a balanced mix of signal processing and summary statistics elements. Specifically, from the signal processing category, the gripper speed average length emerges as the most significant feature, followed by the gripper speed command correlation coefficient median, ranking as the fourth most important, highlighting the role of gripper movement clusters in the classification process. On the other hand, from the summary statistics category, the total number of incoming packets and the 20th percentile of outgoing packet inter-arrival times stand out as the second and third most important features, respectively. This highlights that different classes exhibit variations not only in the total number of packets sent but also in the timing between these packets. Such distinctions enable our classifier to correctly distinguish between classes. We refer the reader to Appendix C – Figure 17 for a comprehensive list of these features and their absolute importance values, and deliver a closer visualization and discussion of how different robot commands differ between actions in Appendix F.

7 TOWARDS EFFICIENT DEFENSES

Here, we explore different defense mechanisms and determine their effectiveness in protecting robotic operations from traffic analysis attacks. We evaluate two types of defenses: one based on the simple *padding of packet sizes*, and a more complex one developed by ourselves, which we named *latency-aware traffic modulation*.

At the core of the defense mechanisms we consider lies a concern over how these defenses may impact the correct and timely

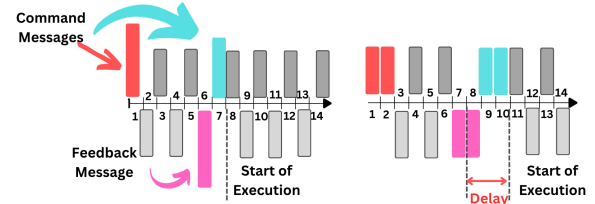


Figure 11: Accumulative delay in robotic action execution.

operation of the robot. As it stands, the robot can only proceed with another action after it has received an entire command message and feedback messages about that same command (both possibly segmented over multiple packets). Delaying this cycle would lead to delays in action execution, as illustrated in the simplification presented in Figure 11, where red and blue colored packets represent different command messages, and purple colored packets represent feedback messages. In this example, each packet is sent after a fixed time interval. The left part of the figure shows the original traffic trace, while the right part illustrates the traffic post-segmentation, where all packets are broken down into a uniform size and where the delivery of command and feedback messages is delayed due to the segmentation. To ensure that action correctness and operational efficiency is maintained, the content within the command and feedback messages must be sequentially delivered before any robotic action can be executed. Moreover, the messages exchanged between the robot and the controller while a command’s execution is ongoing (indicated by gray bars) should also not be delayed.

7.1 Considered Defenses

Padding packet sizes. This defense involves rounding up each packet size to the nearest hundredth, such as to 200 bytes or 800 bytes. This approach aims to obfuscate the actual size of the packets, making it more challenging for an adversary to discern patterns based on packet size. This method does not introduce any additional latency, as it does not affect the transmission time of the packets. However, it does result in additional bandwidth overhead due to the transmission of larger-sized packets.

Latency-aware traffic modulation. This defense strategy is inspired by constant-rate traffic analysis defenses (in the likes of CS-BuFLO [5] or Tamaraw [6]), which involve the use of a fixed packet size for all messages. Generically, applying such a defense to our setting would cause the segmentation of any robot command or feedback message larger than this fixed size into several packets of equal size, or, alternatively, the padding of the contents of small messages to meet this fixed packet size. Then, all packets would be sent at a specific and fixed time interval.

However, the above method can introduce delays, particularly if the frequency of packet transmission does not align with the speed at which the robot’s controller operates. Concretely, the Kinova Gen3 robotic arm features a closed-loop control system operating at a frequency of 1 kHz. Our analysis of the robot operation traffic revealed that the command message type with the *shortest inter-packet intervals* is the speed command, which averages about 80 packets per second. Any latency in a single command/feedback message that results in the message arriving noticeably late to the controller is unacceptable.

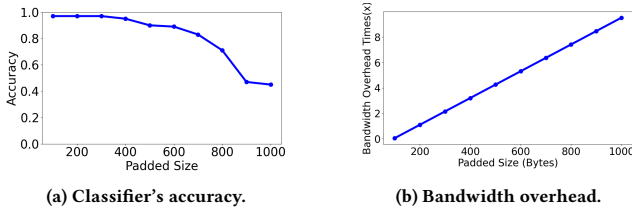


Figure 12: Results for the padding-only defense.

To address this, we developed a *latency-aware traffic modulation* scheme that helps maintain latency within an acceptable range while adequately obfuscating traffic patterns. Like constant-rate defenses, our technique still relies on sending dummy packets to fulfill fixed packet sending rates and padding short packets to meet the pre-configured fixed packet size. However, we leave packets longer than this fixed size (and which cannot be broken down without exceeding the acceptable latency range) at their original size. In turn, packets that can be segmented into multiple smaller packets without resulting in unacceptable delays are appropriately split. This approach still introduces some latency, but can keep it within an acceptable range for the robotic arm’s operation [27].

As a concrete formulation, let s_o be the original packet size, and let s_p be the predefined padded packet size. Let L be the permissible latency 0.001 second in the case of running the Kinova controller and t_i be the chosen time interval for transmitting each packet. The calculated packet size s_c and the number of segments n into which the original packet is divided can be defined as follows:

$$s_c = \begin{cases} s_p & \text{if } s_o \leq s_p, \\ \left\lceil \frac{s_o}{\lfloor \frac{L}{t_i} \rfloor} \right\rceil & \text{if } \left\lceil \frac{s_o}{s_p} \right\rceil \cdot t_i > L, \\ s_p & \text{otherwise.} \end{cases} \quad (1)$$

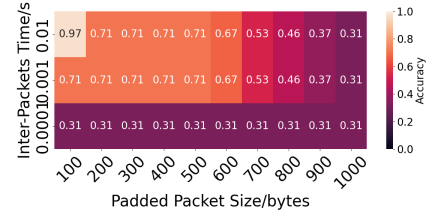
The number of segments n is given by:

$$n = \begin{cases} 1 & \text{if } s_o \leq s_p, \\ \left\lceil \frac{L}{t_i} \right\rceil & \text{if } \left\lceil \frac{s_o}{s_p} \right\rceil \cdot t_i > L, \\ \left\lceil \frac{s_o}{s_p} \right\rceil & \text{otherwise.} \end{cases} \quad (2)$$

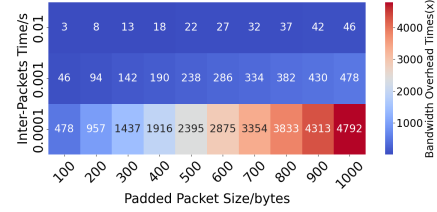
Here, $\lceil \cdot \rceil$ denotes the ceiling and $\lfloor \cdot \rfloor$ denotes the floor function.

7.2 Evaluation of Defenses

Padding-only defense. Figure 12a illustrates the relationship between the accuracy of our classifier and the size of padded packets when the simpler padding-only defense is employed. We can see that the classifier retains a relatively high accuracy (above 80%) for packets padded until a maximum of 700 bytes, decreasing its accuracy to ~40% when packets are padded to 1000 bytes. For analyzing the security/efficiency trade-off in more detail, Figure 12b depicts the average bandwidth overhead percentage of the defense when considering our robot actions dataset. As observed, the overhead percentage increases linearly with the padding size, reaching approximately 700% overhead when the padding size is set to 800 bytes. At this padding size, the classification accuracy of our classifier is still relatively high (~70%). Thus, we conclude that this



(a) Classifier's accuracy.



(b) Bandwidth overhead.

Figure 13: Results for the latency-aware defense.

defense is largely ineffective for low padding sizes, achieving only a moderate protection for a large bandwidth overhead.

Latency-aware traffic modulation defense. For evaluating this defense, we perform a set of experiments with different permissible latency: 0.01s, matching the fastest average command speed, specifically for speed commands; 0.001s, aligning with the controller’s operational frequency, and; 0.0001s, the frequency allowing the transmission of the shortest command/feedback message. While the speed command typically exhibits the fastest average frequency, some command messages contain packets with significantly smaller single inter-packet intervals.

Figure 13a illustrates the relationship between the effectiveness of our defense mechanism and the degree of packet padding and segmentation applied to robot traffic. We can see that, for fixed packet sending rates of 0.01s and 0.001s, the defense is only reasonably effective once packets are also padded to a large size (900 bytes for degrading classification accuracy below 40%). However, we can also see that, for all the padding sizes under test, sending packets at a fixed frequency of 0.0001s is sufficient for reducing the accuracy of the classifier to approximately 30%. Thus, these results suggest that our obfuscation approach can effectively thwart the correct recognition of robot actions by obfuscating the packet sizes and timing patterns that would allow an adversary to correctly recognize commands. Figure 13a also suggests that an adversary may however still be able to infer information about the actions being performed (with an accuracy of ~30%) due to the total time duration of each action (which our technique does not obfuscate).

Figure 13b illustrates the bandwidth overhead incurred by the latency-aware traffic modulation defense. We can see from the figure that bandwidth overhead increases both with the packet size used in the defense and with the increase in packet sending frequency. The figure suggests that the latter cause more pronounced bandwidth overhead, given the larger number of packets exchanged per unit of time. When sending packets at a 0.01s rate, the latency-aware defense is able to reduce our attack’s accuracy to 31% but incurs a staggering 478 times bandwidth overhead. Unfortunately, this

trade-off is not practical in realistic settings, indicating a pressing need for the development of more sophisticated low-delay defense strategies that can provide robust privacy protections. Reasoning about such defenses is a compelling direction for future work.

8 LIMITATIONS AND FUTURE WORK

This section discusses the limitations of our study and points to several directions for future work.

Analysis of teleoperation traffic. In this study, we focused on script-based control of collaborative robotic arms and analyzed the traffic patterns generated during various actions. We demonstrated that specific robot operations could be identified through traffic analysis, even when the communications are encrypted. Our future work includes exploring teleoperation scenarios to reconstruct high-level movements from low-level movements, focusing on scenarios similar to the ones considered (e.g. domestic, service applications).

Extension to the open-world setting. Our evaluation resembles that of a closed-world attack in the website fingerprinting literature. Specifically, we attempt to distinguish between a restricted set of four different actions performed by the robot. In the future, we aim to analyze the effectiveness of our approach in the open-world setting, where the robot is allowed to perform a vast range of tasks which the adversary is unaware of, and where the task of the adversary is to determine whether the action being performed is within the set of the four considered actions (and if so, which one).

Traffic analysis under varying network conditions. In our study, we assumed the existence of a stable and high-performance network connection which was free from interference (e.g., packet drops, jitter, etc. caused by adversarial behavior or network malfunctions). An interesting direction for future work would be to consider the traffic analysis of robot traffic under varying network conditions. Different network environments may introduce unique challenges and opportunities for attack and defense strategies. We plan to create a better understanding of these dynamics towards developing traffic analysis-resistant solutions for robotic systems.

Measuring robot traffic information leakage. We aim to explore more systematic methods for evaluating information leakage in robot traffic [8, 29, 50]. Automating a security evaluation pipeline for robotics applications could also enhance the efficiency and effectiveness of security assessments applied to these systems.

9 RELATED WORK

Traffic analysis has been extensively used for fingerprinting user activities beyond the scenario addressed in this paper. However, the different traffic analysis domains we enumerate below target the re-identification of traffic that follows relatively stable patterns. We argue that the fingerprinting of robot actions via traffic analysis presents unique challenges – complex robot activities might involve a variable number of smaller operations which can be performed in different orders and where each operation can last for different amounts of time. This variability adds a layer of complexity to traffic analysis, as the same high-level activity could result in vastly different traffic patterns, depending on the specifics of the task at hand. In our work, we rely on a new set of manually-engineered features based on signal processing operations, combining these

with traffic summary statistics that have been successfully used in previous fingerprinting attacks mentioned below.

Website fingerprinting. Despite the use of encrypted tunnels like VPNs and low-latency anonymity networks like Tor [12], web traffic retains characteristic traffic patterns that allow eavesdroppers to map those patterns to specific websites [22]. While the creation of these mappings has traditionally resorted to manual feature engineering [22, 36, 51] and classical machine learning algorithms, recent developments rely on the use of deep learning to improve the accuracy and the efficiency of website fingerprinting attacks [40, 42, 45, 47]. There also exists a prolific literature on website fingerprinting defenses, ranging from rather secure but inefficient constant-rate padding defenses [5, 6], to more efficient defenses like FRONT [20] or RegulaTor [23]. We refer the reader to a more complete exposition and analysis of defenses [31, 54].

Video fingerprinting. Video streaming protocols, such as Dynamic Adaptive Streaming over HTTP (DASH) or HTTP Live Streaming (HLS), which adjust their bit rates in response to varying network conditions, manifest traffic patterns that fluctuate based on the video content and its current quality or resolution. These fluctuations have enabled the development of video streaming fingerprinting techniques which can identify a given video being streamed, even if it is encrypted [1, 21, 41, 43, 53]. Apart from enabling attackers to breach through users' privacy [39], encrypted video fingerprinting techniques could enhance existing initiatives for enforcing digital rights management and online content tracking [30]. Proposed defenses include the generation of synthetic video flows that shield the actual videos being watched by users [49], or the introduction of noise to decrease classification accuracy [28].

IoT device fingerprinting. IoT devices typically exhibit regular and predictable traffic patterns which are only partially shrouded by encryption, enabling eavesdroppers to infer which specific devices operate within a smart-household [3]. Worse yet, once a device is identified, eavesdroppers may be able to learn more potentially sensitive information. For example, lack of activity by a previously identified motion sensor may telltale the absence of users within a household. Similarly to website fingerprinting, different approaches for IoT device fingerprinting have focused both on the collection of summary statistics from IoT device traffic [9, 32, 48], or on the analysis of network traces with deep neural networks [13]. Existing defenses include improved padding schemes [14] and the perturbation of traffic flows through deep learning methods [34, 46].

10 CONCLUSION

In this paper, we investigated encrypted traffic analysis in robotics, emphasizing its implications for sensitive applications (e.g., domestic, healthcare, and service). Leveraging machine learning, we were able to discern robotic actions from encrypted traffic patterns, shedding light on significant privacy concerns. Our findings highlight potential vulnerabilities within robotic communication channels, calling for the development of enhanced security measures as the deployment of collaborative robots becomes widespread. While this study advances our understanding of the above issues, future work should focus on devising stronger and more efficient defense mechanisms in the realm of collaborative robotics security.

REFERENCES

- [1] Waleed Afandi, Syed Muhammad Ammar Hassan Bukhari, Muhammad US Khan, Tahir Maqsood, and Samee U Khan. 2022. Fingerprinting technique for youtube videos identification in network traffic. *IEEE Access* 10 (2022), 76731–76741.
- [2] Khaled Al-Naami, Swarup Chandra, Ahmad Mustafa, Latifur Khan, Zhiqiang Lin, Kevin Hamlen, and Bhavani Thuraisingham. 2016. Adaptive encrypted traffic fingerprinting with bi-directional dependence. In *Proceedings of the 32nd Annual Conference on Computer Security Applications*. 177–188.
- [3] Noah Aporthe, Dillon Reisman, and Nick Feamster. 2016. A smart home is no castle: Privacy vulnerabilities of encrypted IoT traffic. In *Proceedings of the Workshop on Data and Algorithmic Transparency*.
- [4] Diogo Barradas, Nuno Santos, and Luis Rodrigues. 2018. Effective Detection of Multimedia Protocol Tunneling using Machine Learning. In *Proceedings of the 27th USENIX Security Symposium*. 169–185.
- [5] Xiang Cai, Rishab Nithyanand, and Rob Johnson. 2014. Cs-bufl0: A congestion sensitive website fingerprinting defense. In *Proceedings of the 13th Workshop on Privacy in the Electronic Society*. 121–130.
- [6] Xiang Cai, Rishab Nithyanand, Tao Wang, Rob Johnson, and Ian Goldberg. 2014. A systematic approach to developing and evaluating website fingerprinting defenses. In *Proceedings of the 2014 ACM SIGSAC Conference on Computer and Communications Security*. 785–794.
- [7] Tianqi Chen and Carlos Guestrin. 2016. Xgboost: A scalable tree boosting system. In *Proceedings of the 22nd acm sigkdd international conference on knowledge discovery and data mining*. 785–794.
- [8] Giovanni Cherubin. 2017. Bayes, not Naïve: Security Bounds on Website Fingerprinting Defenses. *Proceedings on Privacy Enhancing Technologies* 4 (2017), 135–151.
- [9] Rajarshi Roy Chowdhury, Sandhya Aneja, Nagender Aneja, and Emeroylariffion Abas. 2020. Network traffic analysis based iot device identification. In *Proceedings of the 2020 4th International Conference on Big Data and Internet of Things*. 79–89.
- [10] Giovanni Colucci, Luigi Tagliavini, Luca Carbonari, Paride Cavallone, Andrea Botta, and Giuseppe Quaglia. 2021. Paquitop. arm, a mobile manipulator for assessing emerging challenges in the COVID-19 pandemic scenario. *Robotics* 10, 3 (2021), 102.
- [11] Tamara Denning, Cynthia Matuszek, Karl Koscher, Joshua R Smith, and Tadayoshi Kohno. 2009. A spotlight on security and privacy risks with future household robots: attacks and lessons. In *Proceedings of the 11th international conference on Ubiquitous computing*. 105–114.
- [12] Roger Dingledine, Nick Mathewson, and Paul Syverson. 2004. Tor: The Second-generation Onion Router. In *Proceedings of the 13th Conference on USENIX Security Symposium*. 303–321.
- [13] Shuaike Dong, Zhou Li, Di Tang, Jiongyi Chen, Menghan Sun, and Kehuan Zhang. 2020. Your smart home can't keep a secret: Towards automated fingerprinting of iot traffic. In *Proceedings of the 15th ACM Asia Conference on Computer and Communications Security*. 47–59.
- [14] Aviv Engelberg and Avishai Wool. 2022. Classification of encrypted IoT traffic despite padding and shaping. In *Proceedings of the 21st Workshop on Privacy in the Electronic Society*. 1–13.
- [15] European Union Agency for Cybersecurity (ENISA). 2019. Encrypted Traffic Analysis. <https://www.enisa.europa.eu/publications/encrypted-traffic-analysis>. Accessed: 25 November 2023.
- [16] Paolo Fiorini, Ken Y Goldberg, Yunhui Liu, and Russell H Taylor. 2022. Concepts and trends in autonomy for robot-assisted surgery. *Proc. IEEE* 110, 7 (2022), 993–1011.
- [17] Reinaldo Padilha França, Ana Carolina Borges Monteiro, Rangel Arthu, and Yuzo Iano. 2020. The evolution of robotic systems: Overview and its application in modern times. *Safety, Security, and Reliability of Robotic Systems* (2020), 1–20.
- [18] Giuseppe Gillini, Paolo Di Lillo, Filippo Arrichiello, Daniele Di Vito, Alessandro Marino, Gianluca Antonelli, and Stefano Chiaverini. 2022. A dual-arm mobile robot system performing assistive tasks operated via p300-based brain computer interface. *Industrial Robot: the international journal of robotics research and application* 49, 1 (2022), 11–20.
- [19] Aaron Gong. 2022. Website Fingerprinting Repository. <https://github.com/websitefingerprinting/WebsiteFingerprinting> GitHub repository.
- [20] Jiajun Gong and Tao Wang. 2020. Zero-delay lightweight defenses against website fingerprinting. In *Proceedings of the 29th USENIX Security Symposium*. 717–734.
- [21] J. Gu, J. Wang, Z. Yu, and K. Shen. 2018. Walls Have Ears: Traffic-based Side-channel Attack in Video Streaming. In *Proceedings of the 37th IEEE Conference on Computer Communications*. 1538–1546.
- [22] Jamie Hayes and George Danezis. 2016. k-fingerprinting: A Robust Scalable Website Fingerprinting Technique. In *Proceedings of the 25th USENIX Security Symposium*. 1187–1203.
- [23] James K. Holland and Nicholas Hopper. 2022. RegulaTor: A Straightforward Website Fingerprinting Defense. *Proceedings on Privacy Enhancing Technologies* 2022, 2, 344–362.
- [24] Xi Jiang, Shinan Liu, Aaron Gember-Jacobson, Arjun Nitin Bhagoji, Paul Schmitt, Francesco Bronzino, and Nick Feamster. 2023. NetDiffusion: Network Data Augmentation Through Protocol-Constrained Traffic Generation. arXiv:2310.08543 [cs.NI]
- [25] Parham M Kebria, Hamid Abdi, Mohsen Moradi Dalvand, Abbas Khosravi, and Saeid Nahavandi. 2018. Control methods for internet-based teleoperation systems: A review. *IEEE Transactions on Human-Machine Systems* 49, 1 (2018), 32–46.
- [26] Kinova Robotics. 2023. Kinova Gen3 Robotic Arm. <https://www.kinovarobotics.com/product/gen3-robots>. Accessed: 29 November 2023.
- [27] Kinova Robotics. 2023. Kinova Gen3 Specifications. <https://www.kinovarobotics.com/product/gen3-robots>. Accessed: 29 November 2023.
- [28] Haipeng Li, Ben Niu, and Boyang Wang. 2020. SmartSwitch: Efficient Traffic Obfuscation Against Stream Fingerprinting. In *Security and Privacy in Communication Networks*. Springer International Publishing, 255–275.
- [29] Shuai Li, Huajun Guo, and Nicholas Hopper. 2018. Measuring information leakage in website fingerprinting attacks and defenses. In *Proceedings of the 2018 ACM SIGSAC Conference on Computer and Communications Security*. 1977–1992.
- [30] Jian Lu. 2009. Video fingerprinting for copy identification: from research to industry applications. *Media Forensics and Security* 7254 (2009), 725402.
- [31] Nate Mathews, James K Holland, Se Eun Oh, Mohammad Saidur Rahman, Nicholas Hopper, and Matthew Wright. 2023. SoK: A critical evaluation of efficient website fingerprinting defenses. In *Proceedings of the 44th IEEE Symposium on Security and Privacy*. 969–986.
- [32] Nizar Msadek, Ridha Soua, and Thomas Engel. 2019. IoT Device Fingerprinting: Machine Learning based Encrypted Traffic Analysis. In *Proceedings of the 2019 IEEE Wireless Communications and Networking Conference*. 1–8.
- [33] Milad Nasr, Amir Houmansadr, and Arya Mazumdar. 2017. Compressive traffic analysis: A new paradigm for scalable traffic analysis. In *Proceedings of the 2017 ACM SIGSAC Conference on Computer and Communications Security*. 2053–2069.
- [34] Santosh Nukavarapu and Tamer Nadeem. 2022. iKnight-Guarding IoT Infrastructure Using Generative Adversarial Networks. *IEEE Access* 10 (2022), 132656–132674.
- [35] Edwin Daniel Oña, Juan Miguel Garcia-Haro, Alberto Jardón, and Carlos Balaguer. 2019. Robotics in health care: Perspectives of robot-aided interventions in clinical practice for rehabilitation of upper limbs. *Applied sciences* 9, 13 (2019), 2586.
- [36] Andriy Panchenko and Fabian Lanze. 2016. Website Fingerprinting at Internet Scale. In *Proceedings of the 23rd Network and Distributed System Security Symposium*.
- [37] Terrin Babu Pulikottil, Marco Caimmi, Maria Grazia D'Angelo, Emilia Biffi, Stefania Pellegrinelli, and Lorenzo Molinari Tosatti. 2018. A voice control system for assistive robotic arms: preliminary usability tests on patients. In *2018 7th IEEE International Conference on Biomedical Robotics and Biomechatronics (Biorob)*. 167–172.
- [38] Morgan Quigley, Ken Conley, Brian Gerkey, Josh Faust, Tully Foote, Jeremy Leibs, Rob Wheeler, Andrew Y Ng, et al. 2009. ROS: an open-source Robot Operating System. In *ICRA workshop on open source software*, Vol. 3. 5.
- [39] Mohammad Saidur Rahman, Nate Mathews, and Matthew Wright. 2019. Poster: video fingerprinting in tor. In *Proceedings of the 2019 ACM SIGSAC Conference on Computer and Communications Security*. 2629–2631.
- [40] Mohammad Saidur Rahman, Payap Sirinam, Nate Mathews, Kantha Girish Gangadhara, and Matthew Wright. 2020. Tik-Tok: The utility of packet timing in website fingerprinting attacks. In *Proceedings on Privacy Enhancing Technologies (PoPETs)*, Vol. 2020. 5–24. Issue 3.
- [41] Andrew Reed and Michael Kranch. 2017. Identifying HTTPS-Protected Netflix Videos in Real-Time. In *Proceedings of the 7th ACM on Conference on Data and Application Security and Privacy*. 361–368.
- [42] Vera Rimmer, Davy Preuveneers, Marc Juarez, Tom Van Goethem, and Wouter Joosen. 2018. Automated website fingerprinting through deep learning. In *Proceedings of the 25th Network and Distributed Systems Security Symposium*.
- [43] Roei Schuster, Vitaly Shmatikov, and Eran Tromer. 2017. Beauty and the burst: Remote identification of encrypted video streams. In *Proceedings of the 26th USENIX Security Symposium*. 1357–1374.
- [44] Ryan Shah, Chuadhry Mujeeb Ahmed, and Shishir Nagaraja. 2022. Can You Still See Me?: Identifying Robot Operations Over End-to-End Encrypted Channels. In *Proceedings of the 15th ACM Conference on Security and Privacy in Wireless and Mobile Networks*. 298–300.
- [45] Meng Shen, Kexin Ji, Zhenbo Gao, Qi Li, Liehuang Zhu, and Ke Xu. 2023. Subverting Website Fingerprinting Defenses with Robust Traffic Representation. In *Proceedings of the 32nd USENIX Security Symposium*. 607–624.
- [46] Akshaye Sheno, Prasanna Karthik, Kanav Sabharwal, Li Jialin, and Dinil Mon Divakaran. 2023. iPET: Privacy Enhancing Traffic Perturbations for IoT Communications. *Proceedings on Privacy Enhancing Technologies* (2023).
- [47] Payap Sirinam, Mohsen Imani, Marc Juarez, and Matthew Wright. 2018. Deep fingerprinting: Undermining website fingerprinting defenses with deep learning. In *Proceedings of the 2018 ACM SIGSAC Conference on Computer and Communications Security*. 1928–1943.
- [48] Monika Skowron, Artur Janicki, and Wojciech Mazurczyk. 2020. Traffic fingerprinting attacks on internet of things using machine learning. *IEEE Access* 8

(2020), 20386–20400.

- [49] Alexander Vaskevich, Thilini Dahanayaka, Guillaume Jourjon, and Suranga Seneviratne. 2021. SMAUG: Streaming Media Augmentation Using CGANs as a Defence Against Video Fingerprinting. In *Proceedings of the 20th IEEE International Symposium on Network Computing and Applications*. 1–10.
- [50] Alexander Veicht, Cedric Renggli, and Diogo Barradas. 2023. DeepSE-WF: Unified Security Estimation for Website Fingerprinting Defenses. *Proceedings on Privacy Enhancing Technologies* Vol. 2 (2023), 188–205.
- [51] Tao Wang, Xiang Cai, Rishab Nithyanand, and Rob Johnson. 2014. Effective Attacks and Provable Defenses for Website Fingerprinting. In *Proceedings of the 23rd USENIX Security Symposium*. 143–157.
- [52] Garrett Wilson, Christopher Pereyda, Nisha Raghunath, Gabriel de la Cruz, Shivam Goel, Sepehr Nesaei, Bryan Minor, Maureen Schmitter-Edgecombe, Matthew E Taylor, and Diane J Cook. 2019. Robot-enabled support of daily activities in smart home environments. *Cognitive Systems Research* 54 (2019), 258–272.
- [53] Hua Wu, Zhenhua Yu, Guang Cheng, and Shuyi Guo. 2020. Identification of encrypted video streaming based on differential fingerprints. In *IEEE INFOCOM 2020-IEEE Conference on Computer Communications Workshops (INFOCOM WK-SHPS)*. 74–79.
- [54] Xi Xiao, Xiang Zhou, Zhenyu Yang, Le Yu, Bin Zhang, Qixu Liu, and Xiapu Luo. 2023. A Comprehensive Analysis of Website Fingerprinting Defenses on Tor. *Computers & Security* (2023), 103577.
- [55] Yucheng Yin, Zinan Lin, Minhao Jin, Giulia Fanti, and Vyasa Sekar. 2022. Practical gan-based synthetic ip header trace generation using netshare. In *Proceedings of the ACM SIGCOMM 2022 Conference*. 458–472.

A KINOVA ROBOTIC ARM PLATFORM

Figure 14 depicts the Kinova Robotics arm Gen 3 model we leverage in our experiments.



Figure 14: Photo of the Kinova Gen3 robotics arm.

B COMMAND-SPECIFIC TRAFFIC PATTERNS

This section provides additional details on different kinds of commands we leverage for producing the robotic actions considered in our dataset. Concretely, we provide additional details for commands regarding *angular motion* and *gripper speed*.

Angular motion commands. These commands involve adjusting the robot arm’s joints to specific angles, exhibit a different yet conceptually similar traffic pattern. These commands typically involve a one-time pattern but have a longer duration and shorter ingoing packet sizes received from the robot. The distinct traffic signature for angular motion is reflective of the precise control required for positioning each joint at a specific angle. A depiction of two different traffic samples of angular motion commands is shown in Figure 15.

Gripper speed commands. These commands control the speed at which the gripper opens or closes, are more frequent and have shorter inter-packet timings. These messages maintain a consistent packet length for both ingoing and outgoing transmissions and last for the duration of the gripper’s movement. This indicates a continuous stream of data necessary to regulate the speed of the gripper’s motion. A depiction of two different traffic samples of gripper speed commands is shown in Figure 16.

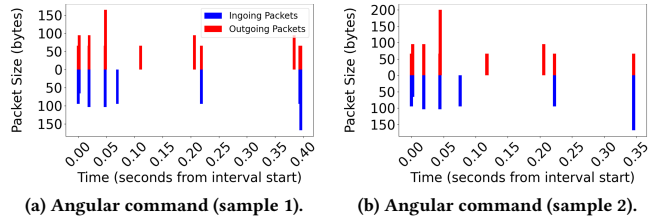


Figure 15: Traces of two different angular commands.

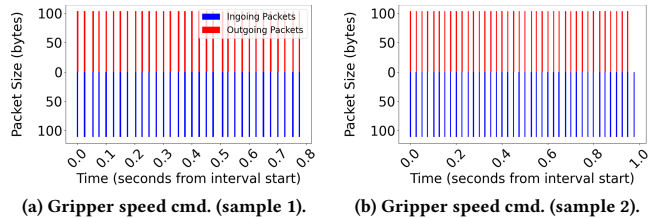


Figure 16: Traces of two different gripper speed commands.

C FEATURE IMPORTANCE

Figure 17 depicts the top 20 most important features considered by our classifier when attempting the identification of robotic actions from encrypted traffic.

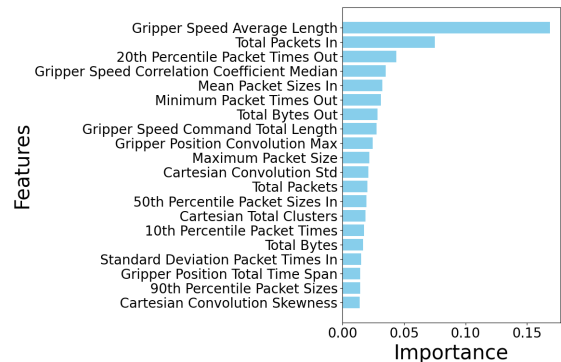


Figure 17: The top 20 most important features.

D CONVOLUTION AND CORRELATION COEFFICIENT FEATURES

Table 3 presents all the features extracted through convolution and correlation coefficient methods.

E COMPLETE SET OF FEATURES

Listing 1 presents a complete list of the features included in our traffic classifier.

1. TotalPackets	Total number of packets in the communication
2. totalPacketsIn	Total number of incoming packets
3. totalPacketsOut	Total number of outgoing packets
4. totalBytes	Total bytes of data in the communication
5. totalBytesIn	Total bytes of incoming data
6. totalBytesOut	Total bytes of outgoing data
7. p10PacketSizesIn	10th percentile incoming network inter-packet size
8. p20PacketSizesIn	20th percentile incoming network inter-packet size
9. p30PacketSizesIn	30th percentile incoming network inter-packet size
10. p40PacketSizesIn	40th percentile incoming network inter-packet size
11. p50PacketSizesIn	50th percentile incoming network inter-packet size
12. p60PacketSizesIn	60th percentile incoming network inter-packet size
13. p70PacketSizesIn	70th percentile incoming network inter-packet size
14. p80PacketSizesIn	80th percentile incoming network inter-packet size
15. p90PacketSizesIn	90th percentile incoming network inter-packet size
16. p10PacketSizesOut	10th percentile outgoing network inter-packet size
17. p20PacketSizesOut	20th percentile outgoing network inter-packet size
18. p30PacketSizesOut	30th percentile outgoing network inter-packet size
19. p40PacketSizesOut	40th percentile outgoing network inter-packet size
20. p50PacketSizesOut	50th percentile outgoing network inter-packet size
21. p60PacketSizesOut	60th percentile outgoing network inter-packet size
22. p70PacketSizesOut	70th percentile outgoing network inter-packet size
23. p80PacketSizesOut	80th percentile outgoing network inter-packet size
24. p90PacketSizesOut	90th percentile outgoing network inter-packet size
25. minPacketSize	Minimum packet size observed
26. maxPacketSize	Maximum packet size observed
27. meanPacketSizes	Mean size of packets
28. stdevPacketSizes	Standard deviation of packet sizes
29. variancePacketSizes	Variance of packet sizes
30. p10PacketTimesIn	10th percentile incoming network inter-packet timing
31. p20PacketTimesIn	20th percentile incoming network inter-packet timing
32. p30PacketTimesIn	30th percentile incoming network inter-packet timing
33. p40PacketTimesIn	40th percentile incoming network inter-packet timing
34. p50PacketTimesIn	50th percentile incoming network inter-packet timing
35. p60PacketTimesIn	60th percentile incoming network inter-packet timing
36. p70PacketTimesIn	70th percentile incoming network inter-packet timing
37. p80PacketTimesIn	80th percentile incoming network inter-packet timing
38. p90PacketTimesIn	90th percentile incoming network inter-packet timing
39. p10PacketTimesOut	10th percentile outgoing network inter-packet timing
40. p20PacketTimesOut	20th percentile outgoing network inter-packet timing
41. p30PacketTimesOut	30th percentile outgoing network inter-packet timing
42. p40PacketTimesOut	40th percentile outgoing network inter-packet timing
43. p50PacketTimesOut	50th percentile outgoing network inter-packet timing
44. p60PacketTimesOut	60th percentile outgoing network inter-packet timing
45. p70PacketTimesOut	70th percentile outgoing network inter-packet timing
46. p80PacketTimesOut	80th percentile outgoing network inter-packet timing
47. p90PacketTimesOut	90th percentile outgoing network inter-packet timing
48. maxPacketTimesIn	Max time between incoming packets
49. meanPacketTimesIn	Mean time between incoming packets
50. minPacketTimesIn	Minimum time between incoming packets
51. stdevPacketTimesIn	Standard deviation of time between incoming packets
52. variancePacketTimesIn	Variance of time between incoming packets
53. skewPacketTimesIn	Skewness of time between incoming packets
54. kurtosisPacketTimesIn	Kurtosis of time between incoming packets
55. maxPacketTimesOut	Maximum time between outgoing packets
56. meanPacketTimesOut	Mean time between outgoing packets
57. minPacketTimesOut	Minimum time between outgoing packets
58. stdevPacketTimesOut	Standard deviation of time between outgoing packets
59. variancePacketTimesOut	Variance of time between outgoing packets
60. skewPacketTimesOut	Skewness of time between outgoing packets
61. kurtosisPacketTimesOut	Kurtosis of time between outgoing packets
62. meanPacketLength	Mean packet length
63. g_position_conv_mean	Mean of convolution results for gripper position
64. g_position_conv_std	Std. dev. of convolution results for gripper position
65. g_position_conv_median	Median of convolution results for gripper position
66. g_position_conv_percentile_25	25th percentile of conv. results for gripper position
67. g_position_conv_percentile_75	75th percentile of conv. results for gripper position
68. g_position_conv_max	Max. of convolution results for gripper position
69. g_position_conv_min	Min. of convolution results for gripper position
70. g_position_conv_skewness	Skewness of convolution results for gripper position
71. g_position_conv_kurtosis	Kurtosis of convolution results for gripper position
72. g_position_total_clusters	Total number of clusters in gripper position
73. g_position_total_time_span	Total time span of clusters in gripper position
74. g_position_average_time_gap	Average time gap between clusters in gripper position
75. cart_conv_mean	Mean of convolution results for Cartesian commands
76. cart_conv_std	Std. dev. of convolution results for Cartesian commands
77. cart_conv_median	Median of convolution results for Cartesian commands
78. cart_conv_percentile_25	25th percentile of conv. results for Cartesian commands
79. cart_conv_percentile_75	75th percentile of conv. results for Cartesian commands
80. cart_conv_max	Maximum of convolution results for Cartesian commands
81. cart_conv_min	Minimum of convolution results for Cartesian commands
82. cart_conv_skewness	Skewness of convolution results for Cartesian commands
83. cart_conv_kurtosis	Kurtosis of convolution results for Cartesian commands
84. cart_total_clusters	Total number of clusters in Cartesian commands
85. cart_total_time_span	Total time span of clusters in Cartesian commands
86. cart_average_time_gap	Average time gap between clusters in Cartesian commands
87. g_position_corr_mean	Mean of correlation coefficients for gripper speed

88. g_position_corr_std	Std. dev. of correlation coefficients for gripper speed
89. g_position_corr_median	Median of correlation coefficients for gripper speed
90. g_position_corr_percentile_25	25th percentile of corr. coefficients for gripper speed
91. g_position_corr_percentile_75	75th percentile of corr. coefficients for gripper speed
92. g_position_corr_max	Maximum of correlation coefficients for gripper speed
93. g_position_corr_min	Minimum of correlation coefficients for gripper speed
94. g_position_corr_skewness	Skewness of correlation coefficients for gripper speed
95. g_position_corr_kurtosis	Kurtosis of correlation coefficients for gripper speed
96. g_position_num_clusters	Total number of clusters detected for gripper speed
97. g_position_total_length	Total length of all clusters for gripper speed
98. g_position_average_length	Average length of clusters for gripper speed
99. g_position_total_time	Total time from the first to the last cluster for gripper speed

Listing 1: Complete set of features and their description.

F FEATURE DISTRIBUTION ANALYSIS

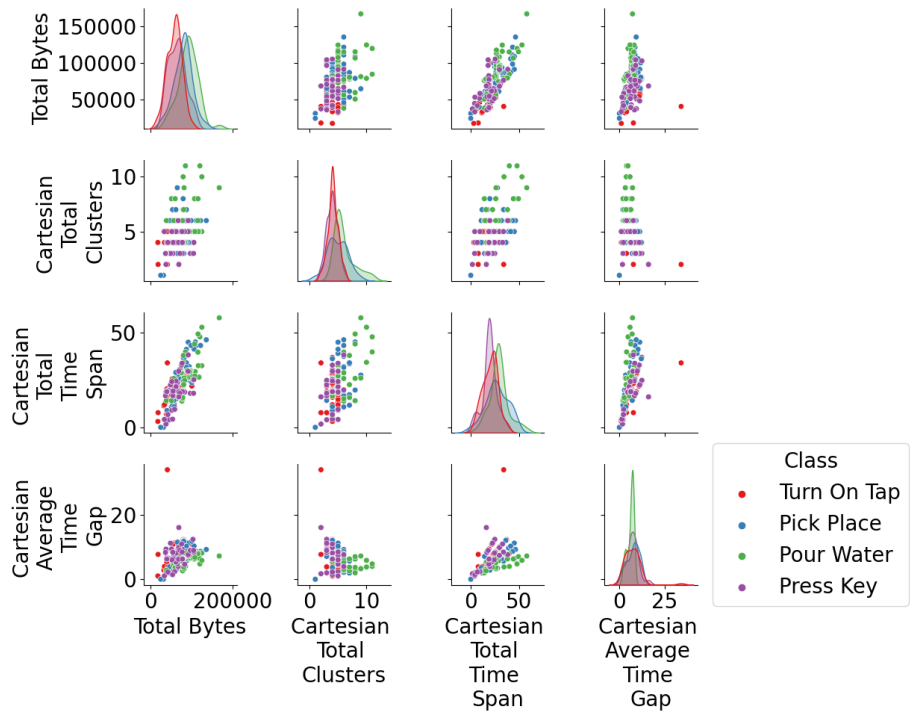
In this section, we aim to showcase the fine-grained disparities between traffic features amongst the robot actions considered in our dataset. Specifically, we show and analyze the pairwise relationship between different features of the robotic actions regarding the execution of cartesian and gripper speed commands.

Cartesian commands. Figure 18a shows the pairwise relationship between different features of the robotic actions considered in our dataset, when focusing Cartesian commands. We observe distinct patterns among different robot actions in terms of total bytes transmitted and the temporal characteristics of the command messages. The actions of pouring water and picking and placing objects tend to involve a larger amount of bytes, indicative of longer durations and more complex movements. In contrast, actions such as pressing a key and turning on a switch, which typically involve simpler tapping motions, are characterized by fewer bytes transmitted. We also identify other differences between actions. For instance, the action of pouring water is marked by a lower average time gap between Cartesian messages and a higher total number of Cartesian clusters, suggesting a more frequent rate of command transmission over a given period. This contrasts with the pick and place action, which, although also characterized by a long total Cartesian time span, exhibits longer average gaps between messages and fewer total clusters. This implies that Cartesian commands are sent less frequently and take longer to execute for the pick and place action. In simpler tapping actions like turning on a tap or pressing a key, the reduced complexity of the movement is reflected in a lower number of total Cartesian clusters and total bytes.

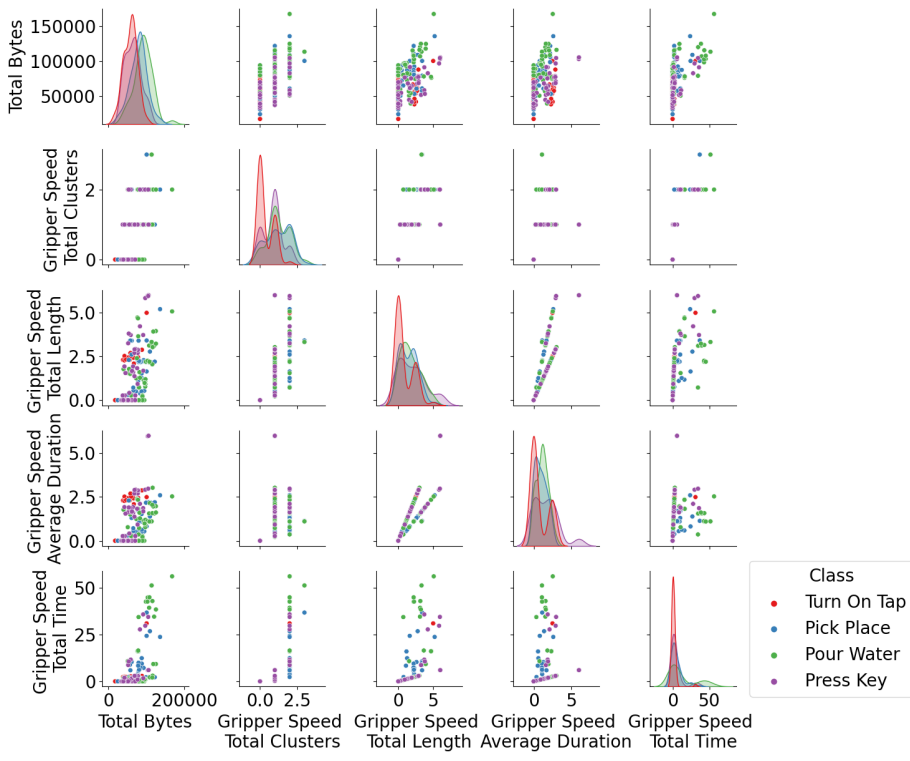
Gripper speed commands. Similarly to the above, Figure 18b reveals noticeable disparities in the number of gripper speed commands performed during the execution of different robot actions. For instance, the “turn on switch” action features significantly fewer gripper speed commands, which aligns with its non-manipulative nature, though it may still involve closing the gripper to facilitate the toggling action. This distinction is further exemplified by the observation that the ‘press key’ and “turn on switch” actions exhibit higher variance and a bimodal distribution in terms of the average duration and total length of gripper speed commands. This contrasts with the unimodal distribution observed for the “pick and place” and “pour water” actions, suggesting a more predictable and consistent pattern of gripper movements for these latter actions.

Metric	Description
Convolution Mean	The average value of the convolution result, indicating the general level of match between the signal and the kernel.
Convolution Standard Deviation	Measures the spread of the convolution results, indicating the variability in the signal's match to the kernel.
Correlation Coefficient Mean	The average of the correlation coefficients, providing an overall measure of how closely the signal matches the kernel pattern.
Correlation Coefficient Standard Deviation	Represents the variability in the correlation coefficients, indicating the consistency of the pattern matches.
Average Timestamps of Clusters	Denotes the mean timing of a group of similar commands or actions. It offers insights into the regularity or frequency of specific activities.
Average Time between Clusters	Represents the average interval between different groups of certain commands, indicating the robot's operational rhythms or periods of inactivity between distinct tasks.
Total Number of Clusters	Indicates the overall count of detected patterns or grouped commands, which aids the understanding the diversity and variability of commands within the captured data.
Total Length of All Clusters	Measures the combined duration of all detected patterns, providing an understanding of the overall time spent by the robot on various grouped actions.
Average Length of Clusters	Signifies the mean duration of each detected pattern, which helps in determining the typical time taken by specific grouped robot activities.
Time Gaps between Consecutive Clusters	Highlights the intervals between successive detected patterns. By examining these gaps, we can infer the potential pauses or transitions between robot activities.
Skewness and Kurtosis	Offer insights into the shape of the convolution result distribution, hinting at the regularity or irregularity of the action.
Total Time Span of Clusters	Shows the difference between the timestamps of the last and first cluster provides insights into the total time frame within which the action occurred.
Average Time Gap between Clusters	Calculates the time gaps between consecutive detected actions (clusters) and then averaging them, revealing the typical interval between repeated actions. This metric can indicate whether the robot is frequently or sporadically performing the action.

Table 3: Summary of convolution and correlation features extracted from the robot action traces.



(a) Cartesian command feature set pairplot.



(b) Gripper speed command feature set pairplot.

Figure 18: Visualization of a selection of cartesian and gripper speed messages's features.